Brief Communication

Chemistry & Biology

Substrate Flexibility of a Mutated Acyltransferase Domain and Implications for Polyketide Biosynthesis

Graphical Abstract

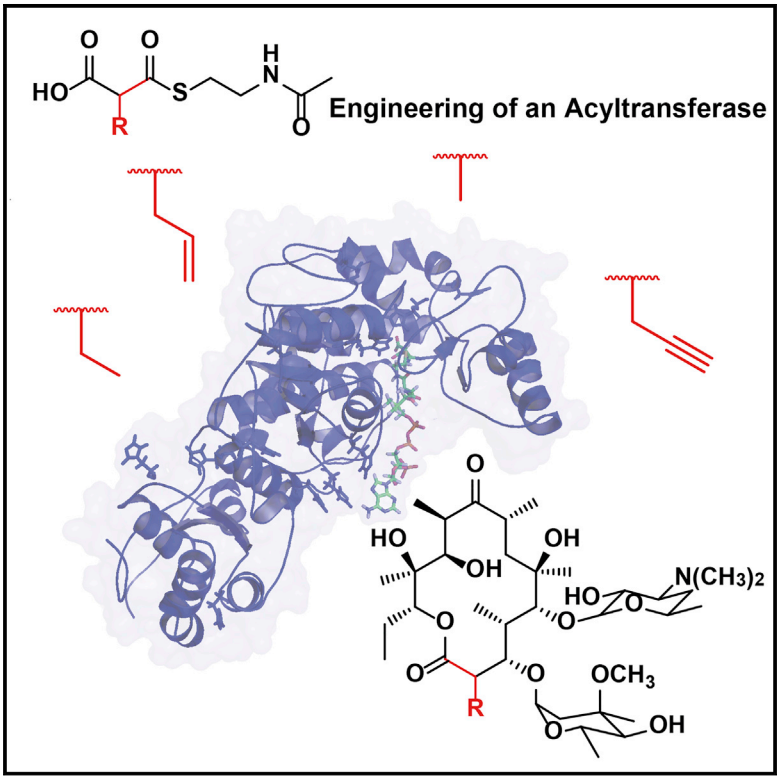

Highlights

- Computational models of a PKS acyltransferase with different substrates are built
- Substrate promiscuity of acyltransferase variants is explored experimentally
- Theory and experiments suggest prediction of AT behavior is possible
- Additional mutations shift substrate scope toward artificial building block

Authors

Kenny Bravo-Rodriguez, Stephan Klopries, Kyra R.M. Koopmans, ..., Susanna Kushnir, Frank Schulz, Elsa Sanchez-Garcia

Correspondence

frank.schulz@rub.de (F.S.), esanchez@mpi-muelheim.mpg.de (E.S.-G.)

In Brief

Molecular modeling of polyketide synthase domains can yield insights into the structure and function of these giant and complex enzymes. Based on modeling, mutations are devised that shift the substrate scope of an acyltransferase domain of a polyketide synthase toward the incorporation of artificial building blocks into the biosynthesis of the important antibiotic erythromycin to generate new derivatives.

Bravo-Rodriguez et al., 2015, Chemistry & Biology *22*, 1425–1430
November 19, 2015
http://dx.doi.org/10.1016/j.chembiol.2015.02.008

CellPress

Chemistry & Biology
Brief Communication

Substrate Flexibility of a Mutated Acyltransferase Domain and Implications for Polyketide Biosynthesis

Kenny Bravo-Rodriguez,[1,5] Stephan Klopries,[2,5] Kyra R.M. Koopmans,[2] Uschi Sundermann,[3] Samir Yahiaoui,[4] Julia Arens,[2] Susanna Kushnir,[2] Frank Schulz,[2,*] and Elsa Sanchez-Garcia[1,*]
[1]Max-Planck-Institut für Kohlenforschung, Kaiser-Wilhelm-Platz 1, 45470 Mülheim an der Ruhr, Germany
[2]Fakultät für Chemie und Biochemie, Organische Chemie 1, Ruhr-Universität Bochum, Universitätsstraße 150, 44780 Bochum, Germany
[3]Dr. Fooke-Achterrath Laboratorien GmbH, Habichtweg 16, 41468 Neuss, Germany
[4]Université de Caen Basse-Normandie, Centre d'Etudes et de Recherche sur le Médicament de Normandie, 14032 Caen, France
[5]Co-first author
*Correspondence: frank.schulz@rub.de (F.S.), esanchez@mpi-muelheim.mpg.de (E.S.-G.)
http://dx.doi.org/10.1016/j.chembiol.2015.02.008

SUMMARY

Polyketides are natural products frequently used for the treatment of various diseases, but their structural complexity hinders efficient derivatization. In this context, we recently introduced enzyme-directed mutasynthesis to incorporate non-native extender units into the biosynthesis of erythromycin. Modeling and mutagenesis studies led to the discovery of a variant of an acyltransferase domain in the erythromycin polyketide synthase capable of accepting a propargylated substrate. Here, we extend molecular rationalization of enzyme-substrate interactions through modeling, to investigate the incorporation of substrates with different degrees of saturation of the malonic acid side chain. This allowed the engineered biosynthesis of new erythromycin derivatives and the introduction of additional mutations into the AT domain for a further shift of the enzyme's substrate scope. Our approach yields non-native polyketide structures with functional groups that will simplify future derivatization approaches, and provides a blueprint for the engineering of AT domains to achieve efficient polyketide synthase diversification.

INTRODUCTION

Polyketides (PKs) are a widespread class of natural products with large pharmaceutical potential (Weissman and Leadlay, 2005). They frequently require structural alterations to become relevant for pharmaceutical applications, highlighting the need for efficient strategies toward their derivatization (Newman and Cragg, 2012). This derivatization is complicated by the structural complexity of PKs that contain a multitude of functional groups and stereogenic centers (Hertweck, 2009).

In bacteria, giant *cis*-acyltransferase type I polyketide synthases (PKSs) catalyze the key steps in the biosynthesis of reduced PKs. In these modular enzymes, ketosynthase, acyltransferase (AT), and acyl carrier protein domains bring about decarboxylative Claisen condensations between an enzyme-bound acyl thioester and the malonic acid-based building blocks used as extender units. In further reductive steps, optional ketoreductase, dehydratase, and enoylreductase domains catalyze the stepwise reduction of the initial β-ketothioester product to a secondary alcohol, olefin, or saturated fatty acid equivalent. The general organization of the biosynthetic machinery is largely conserved among all reduced PKs of bacterial origin, despite a staggering structural variety (Hertweck, 2009).

Aside from alterations in redox pattern and stereochemical configuration of PKs, the use of different biosynthetic building blocks is an important source of diversity in this compound class (Hertweck, 2009; Kushnir et al., 2012; Kwan et al., 2008; Lau et al., 1999; Mo et al., 2010; Oliynyk et al., 1996; Quade et al., 2012). In particular, derivatives of malonic acid-based extender units can be incorporated in different modules of a PKS, adding a potentially high degree of structural flexibility. In nature only a relatively small number of extender units are utilized, in most cases malonyl-coenzyme A (MCoA) and methylmalonyl-CoA (MMCoA). Some AT domains can strictly discriminate between MMCoA and MCoA as substrates, and we recently suggested that the differentiation mechanism between the native substrate MMCoA and the smaller alternative is subtle (Sundermann et al., 2013). The exclusion of completely non-natural substrates does not necessarily have to be strict, as evolutionary pressure on this trait is absent. In experiments with the isolated module 6 of 6-deoxyerythronolide B synthase (DEBS), Koryakina et al. (2013) showed a considerable level of acceptance of differently substituted MCoA derivatives. In special cases, analogous setups also work in vivo (Bravo-Rodriguez et al., 2014; Koryakina et al., 2012).

In our experiments on the biosynthesis of erythromycin in its native producer *Saccharopolyspora erythraea*, no tested artificial extender unit was incorporated into the PK. Apparently, the elevated substrate concentrations required to enforce their acceptance by the PKS cannot be reached in vivo. This result calls for mutagenesis to change the substrate profile of an AT. Intrinsically, such an approach could facilitate targeted and site-specific incorporations with the mutations focused on one

Table 1. Substrates Investigated in This Study

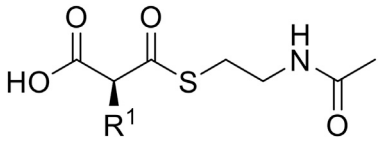

R^1	Compound Name
CH_3	MMSNAC
CH_2CHCH_2	allyl-MSNAC (**1**)
CH_2CCH	propargyl-MSNAC (**2**)
CH_2CH_3	Et-MSNAC (**3**)
$CH(CH_3)_2$	*i*Prop-MSNAC (**4**)
$(CH_2)_3CH_3$	Bu-MSNAC (**5**)
$(CH_2)_5CH_3$	Hex-MSNAC (**6**)
C_6H_5	Ph-MSNAC (**7**)

module, while retaining the specificity of neighboring AT domains.

In our work, we focused on the AT domain in module 6 of DEBS. We employed enzyme-directed mutasynthesis as an approach whereby an AT domain of a PKS is mutated to shift its native substrate profile to a synthetic analog (Sundermann et al., 2013). In contrast to previous approaches, enzyme-directed mutasynthesis is not restricted to starter units of PK biosynthetic pathways and, more importantly, does not rely on the intrinsic substrate promiscuity of a PKS but enforces it through targeted mutagenesis. We found that upon directed mutagenesis of the active site in DEBS AT6, thioester-activated 2-propargylmalonate could serve as an extender unit, leading to 2-propargylerythromycin A. Here, we build on these findings to examine whether active site mutations with different steric demands in comparison with V295 implicated in the earlier work would lower the substrate specificity of the enzyme on a broader basis. We use molecular modeling and feeding experiments with different malonic acid-based building blocks to investigate the enzyme-substrate interactions more precisely. We then translate the improved understanding into mutagenesis experiments to further alter the substrate profile of the enzyme and synthesize new erythromycin derivatives.

RESULTS AND DISCUSSION

For a systematic substrate screening, we synthesized several substituted malonic acid thioesters (compounds **1**–**7** [Table 1]).

Substrate-Free Wild-Type and V295A AT6

Molecular dynamics (MD) simulations of substrate-free wild-type (WT) and V295A AT6 reveal that the V295A mutation results in a wider active site (Figure 1), mainly due to the increased flexibility of the loop containing residue 295. The higher flexibility caused by this mutation also reaches the β-sheet region near Ala295 and the α-helix formed by residues 273–286 (Figure 1). Lastly, the Ala295 side chain can rotate 180° from the Val295 orientation, thereby pointing to the outside of the active site.

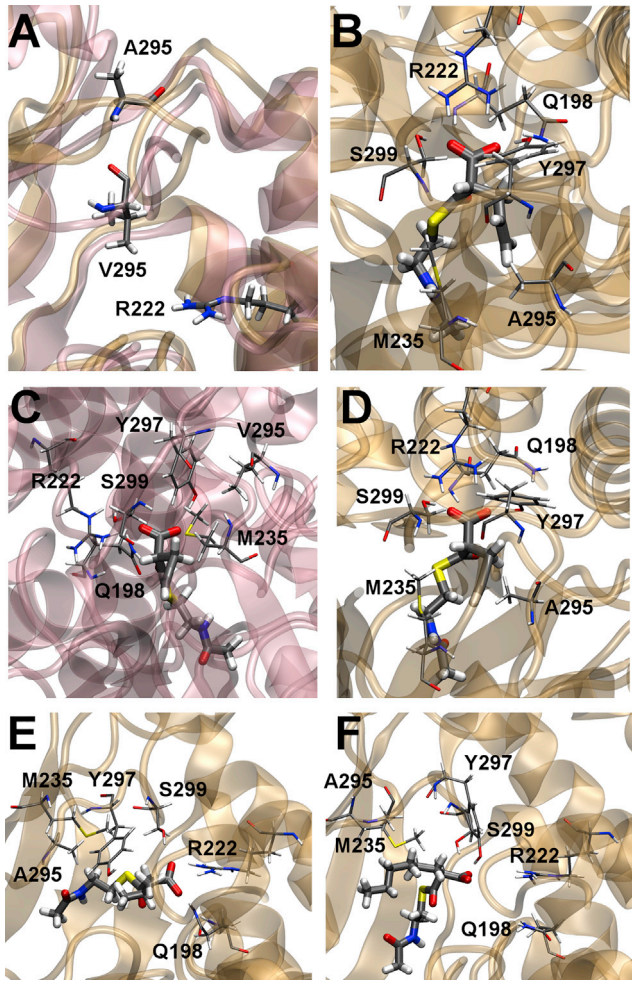

Figure 1. Snapshots of Molecular Dynamics Simulations of the Wild-Type AT6 Domain and of AT6 Carrying the V295A Mutation with Native and Non-native Substrates

(A) Alanine allows for greater flexibility of the binding pocket since this residue adopts positions not accessible to valine (WT-AT6, rose; V295A AT6, ochre).

(B) Allyl-MSNAC (**1**) is placed inside the active site of V295A AT6 with the side group of the malonyl moiety accommodated below Ala295 instead of side by side.

(C) The triple bond of propargyl-MSNAC (**2**) does not readily fit in the active site of WT-AT6. Notice the positioning of Arg222 outside the active site; Met235 and Val295 do not flank the substituent in the malonyl region.

(D) Improved positioning of **2** in the active site of the V295A variant.

(E) V295A AT6 with *iProp*-MSNAC (**4**) and (F) with Hex-MSNAC (**6**).

The substrate is colored according to the atom type, WT-AT6 is colored in rose and V295A AT6 in ochre.

Wild-Type AT6 with Native and Non-native Substrates

To further investigate the origins of substrate specificity, we performed MD simulations of WT-AT6 with the native and two non-native substrates, MMCoA, methylmalonyl-SNAC (MMSNAC), and propargylmalonyl-SNAC (propargyl-MSNAC, **2**), respectively. First, we identified key molecular interactions between WT-AT6 and MMCoA. Our model shows that the carboxylate group of the malonate interacts with Arg222, Tyr297, and Ser299. Gln198 has contacts to the thioester carbonyl group. The side chain on the Cα atom of the substrate is placed between

Met235 and Val295. These two amino acids control both the stereochemistry and the size of the malonic acid side chain. Ser197 is activated by His300 for a nucleophilic attack on the thioester. Therefore, the thioester should come into close contact with Ser197.

MMSNAC features the methylmalonyl moiety, but the thioester region is shorter than in the natural substrate MMCoA. According to previous experiments, WT-AT6 should be able to accept MMSNAC (Klopries et al., 2013). Analysis of the molecular interactions between WT-AT6 and MMSNAC shows little difference compared with WT-AT6-MMCoA in the active site. Since MMSNAC does not feature the CoA fragment, it shows fewer interactions with the solvent-exposed part of the cavity hosting the active site of WT-AT6. This results in a greater mobility of the MMSNAC substrate inside the active site, as evidenced by the lower root-mean-square deviation (RMSD) values of MMCoA with respect to MMSNAC.

The simulations of WT-AT6 in complex with **2** show that the binding is accompanied by major active site rearrangements (Figure 1C and Table S1A). Arg222 is oriented outside of the active site to accommodate **2**, leaving only one NH_2 group of the Arg222 guanidinium moiety to interact with the malonate (Figure 1C). In addition, interactions of Gln198 and Ser299 with the substrate are weakened (Figure 1C and Table S1A) and the triple bond of **2** adopts an unfavorable orientation with respect to Met235 and Val295 (Figure 1C). Our findings are in agreement with a recent report on the incorporation of propargyl-MCoA by DEBS AT6 (Koryakina et al., 2013). In that study, CoA-activated propargylmalonate was used in high concentrations, which cannot be reached in vivo.

Our models of the enzyme-substrate complex show that the correct positioning of the substrate and the conservation of key interactions with the active site are the main factors governing substrate specificity in DEBS AT6. In the presence of high concentrations of non-optimal substrates, purified PKS fragments might accommodate the suitable substrate rotamer to yield the artificial product, as reported by Koryakina et al. (2013).

V295A AT6 with Native and Non-native Substrates

We performed MD simulations with the native substrate bound to V295A AT6 to rationalize its binding mode. The simulations with MMCoA and MMSNAC show that this variant establishes a very similar substrate-active site interaction network as the WT protein (Table S1B). This is in agreement with our previous experimental findings with this enzyme variant, giving rise to a mixture of erythromycin A and 2-propargylerythromycin A from a fermentation supplemented with the artificial building block (Sundermann et al., 2013). The single mutation thus would not switch, but rather relax, the enzyme's substrate specificity.

The MD simulations of V295A AT6 with MMCoA and MMSNAC feature two differences compared with the WT simulations. First, the position of the O atom of MMCoA and MMSNAC shifts with respect to Arg222 (Table S1A). Second, residues Gln113, Gln169, and Gln198 tend to move away from the substrates in all V295A AT6 simulations (Figure 1 and Table S1). Gln113 and Gln169 are not directly involved in interactions with the thioester group of the substrate. Their role in the active site is possibly to contribute to creating a polar environment at the bottom of the active site to aid substrate insertion. Although Gln198 directly interacts with the thioester moiety in the WT-AT6-MMCoA model, previous studies of AT6-Q198A, -Q198P, and -Q198G showed that this is not critical for activity (Sundermann et al., 2013).

V295A AT6 accommodates **2** in the active site (Figure 1A). The simulation of V295A AT6 in complex with **2** indicates its correct positioning (Figure 1D, compare Figure S2D for atoms naming, Table S1B for distances). We found that the increase in loop flexibility in V295A AT6 is important for the accommodation of **2**, and that Ala295 can adopt conformations not accessible to Val295 (Figure 1A).

The simulations of V295A AT6 with bound ethylmalonyl-SNAC (**3**), isopropylmalonyl-SNAC (**4**), and hexylmalonyl-SNAC (**6**) showed that, with a larger substrate side chain, the interactions with the active site become less structured (Figures 1E and 1F). While the MD simulations with **3** display a very similar interaction pattern as the simulations with MMCoA, the models of V295A AT6 bound to **4** show that the bulky isopropyl group cannot be accommodated (Figure 1E). The interaction with Tyr297 is lost and the isopropyl group is not placed between Met235 and Ala295. The carboxylate group of **4** adopts a vertical orientation with respect to the guanidinium moiety of Arg222 (Figure 1E), and the large lateral chain of **6** causes the active site to repel it (Figure 1F and Table S1B).

Furthermore, the incorporation of **1** and phenylmalonyl-SNAC (**7**) was investigated. For **1**, larger distances between Ser197Cα (Ser197OG) and the C atom of the substrate were found: 6.32 ± 0.67 Å (4.25 ± 0.57 Å) (Table S1). However, the Ser197Cα-C distance tends to decrease toward the end of the simulation (values close to 5.0 Å), indicating that Ser197 gets near the substrate. We found that the active site of WT-AT6 accommodates **1** without disrupting any main interactions (Figure 1B and Table S1B).

In the case of **7**, the planar aromatic ring is accommodated with all the key distances in a range of values that makes substrate binding possible, identifying it as a potential substrate (see Table S1B for comparison with MMCoA, MMSNAC, and Et-MSNAC).

Feeding Experiments

Besides the modeled V295A AT6, we tested variants V295L and V295G in feeding experiments using *S. erythraea* NRRL-B-24071. As previously shown, V295A AT6 is capable of producing 2-propargylerythromycin A on an analytical scale, when supplied with **2** in the fermentation medium. Under the same conditions, V295L AT6 only produces erythromycin A, whereas V295G AT6 displays a complete loss of activity (Sundermann et al., 2013). To test whether any of these variants were capable of incorporating non-natural extender units other than **2**, we performed feeding experiments with all derivatives shown in Table 1. Each experiment was carried out with at least four independent clones. Cultures of all variants were supplied with the extender unit analogs in concentrations between 10 and 50 mM. Fermentation extracts were analyzed by liquid chromatography-electrospray ionization mass spectrometry (LC-ESI-MS).

Variant V295G did not give rise to erythromycin A or any derivative at a significant level, indicating that the variant is rendered inactive by the mutation. In comparison with the WT, variant V295L gave rise to lowered amounts of erythromycin A but did

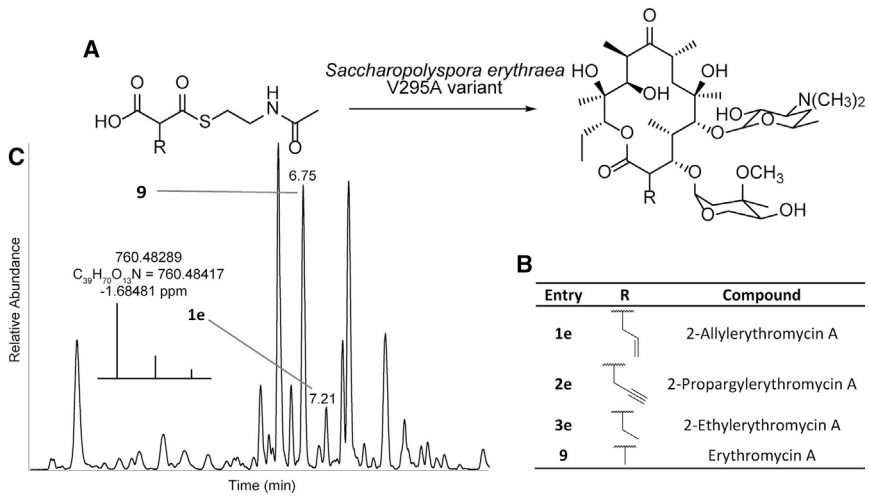

Figure 2. Results of Feeding Experiments with *S. erythraea* DEBS V295A AT6

(A and B) General scheme for the experimental outline. The malonic acid derivatives **1**–**3** were supplied to *S. erythraea* to give rise to the corresponding erythromycin derivatives (see table in B). (C) LC-ESI-MS total ion chromatogram of a fermentation extract from a culture supplied with **1**. It shows the corresponding 2-allylerythromycin A (**1e**) next to the WT product erythromycin A (**9**).

not show significant incorporation levels of any extender unit analog. The WT control experiments also did not give rise to any derivative. Feeding of **7** resulted in diminished cell growth and abolished erythromycin production. Therefore, theoretical prediction of its compatibility with variant V295A could not be experimentally validated.

Upon supplying V295A AT6 with compounds **1**–**7**, analogs **1**–**3** were incorporated into the erythromycin assembly line, **2** serving as positive control. Incorporation was verified by high-resolution MS and tandem MS experiments (Figure 2). V295A AT6 thereby shows significant substrate promiscuity.

Variants supplied with 50 mM of any of the substrates showed no production of either erythromycin A or any of the natural product derivatives, and bacterial growth was diminished. Production levels were significantly lowered at 30 and 40 mM of all tested analogs. Incorporation efficiency was similar for concentrations of 10 and 20 mM of each building block in the medium. The concentration effect was unexpected, as MMSNAC did not show toxicity or any other negative effect in the tested concentration range (Klopries et al., 2013). However, malonic acid thioesters are potent electrophiles, which were recently shown to be able to malonylate electrophilic amino acids in proteins with possible negative effects on the cell's metabolism (Bao et al., 2013).

The concentration effect was reproducible over different batches of the synthetic compounds and over independent clones. Controls with SNAC and the corresponding free malonic acid derivatives revealed a diminished production of erythromycin caused by the free propargylmalonic acid and a sharp decrease of production at a concentration of $\geq$30 mM SNAC. Overall, this result indicates limited opportunities to increase the yield of the fermentation of PK derivatives based solely on precursor-directed biosynthesis.

Simple means such as altered concentrations of the supplied extender unit analogs do not suffice to induce higher yields of the targeted derivatives. Instead, the apparent K_M value of the analog has to be lowered to allow for incorporation at the intracellular concentrations of the building block. The substrate specificity of AT domains must hence be shifted by decreasing acceptance of the native extender unit to lower by-product formation. Based on inspection of the modeled structure of V295A AT6 with bound **2**, we decided to further reduce steric hindrance in the active site through additional mutations. The characteristic YASH motif (Sundermann et al., 2013) was altered to GAGH by site-directed mutagenesis, resulting in a triple variant (V295A, Y297G, S299G). The resulting variant was found to be productive and to yield a significantly higher level of 2-propargylerythromycin (**2e**) relative to the V295A variant (Figure 3).

Comparison of Modeling and Feeding Experiments

The results of the feeding experiments are in agreement with the computational predictions. According to the modeling results, V295A AT6 should be able to accept propargyl, ethyl, allyl, and phenyl side chains. Feeding experiments revealed the synthesis of 2-ethyl- and 2-allylerythromycin A, confirming the acceptance of **3** and **1** as substrates. In agreement with the computational predictions, no isopropyl and hexyl derivatives were detected. The modeled structure of V295A AT6 with bound propargyl-MSNAC suggested that further reduction of steric hindrance in the active site will allow more efficient substrate incorporation. This was experimentally found for a triple variant.

Conclusion

Here, we show that a single mutation causes significant relaxation of the substrate specificity of DEBS AT6. We found that the main requirements on the substrate are the size of the side chain and its flexibility. Hex-MSNAC and *i*Prop-MSNAC are not accepted, whereas propargyl-, Et-, and allyl-MSNAC are. The comparably low incorporation rate is due to the fact that these artificial substrates compete for acceptance with natural MMCoA. In addition, stiff moieties such as the propargyl group should adopt a proper orientation within the AT6 active site. Small flexible building blocks such as Et-MSNAC are accepted similarly to the natural substrate. Theoretical findings show that the incorporation of non-native substrates is favored under the following conditions: (1) close proximity between the thioester group of the substrate and Ser197, (2) substrate side-chain placement between Met235 and Val295, and (3) interaction of Arg222 with the malonate carboxylate group.

With this work, we prove that PKS specificity can be altered by site-directed mutagenesis, and demonstrate how few rationally selected mutations can lead to the incorporation of non-native

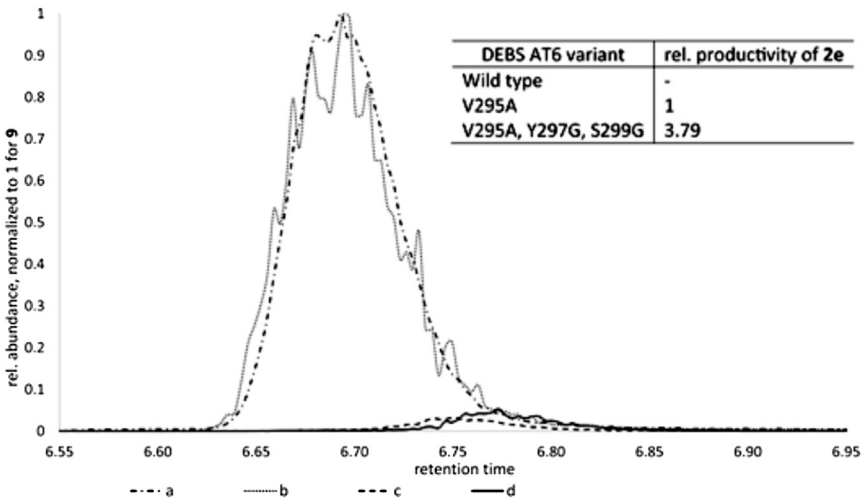

Figure 3. Comparison of V295A AT6 with the New Triple Variant

WT DEBS does not incorporate the synthetic building block **2** in detectable quantities, and V295A AT6 yields low amounts. The triple variant shows a 3.79-fold increase in productivity. For this figure, the abundance of all signals was normalized to **9**, which was set to 1; the chromatogram is shown from 6.55 to 6.95 min. Productivity was quantified based on LC-ESI-MS signals. a, V295A-**9**; b, triple variant **9**; c, V295A **2e**; d, triple variant **2e**.

building blocks. This shows that design principles established in the engineering of small enzymes can be transferred to giant PKS (Kazlauskas, 2005; Morley and Kazlauskas, 2005; Reetz, 2013), but require a thorough enzymological investigation ahead of reaching significant preparative value. In addition, we are able to propose factors regulating AT6 activity. Thus, we provide the first rationalization of substrate incorporation by a PKS, based not only on feeding experiments but also on molecular modeling of enzyme-substrate interactions.

SIGNIFICANCE

Type I PKSs are a large group of biosynthetic enzymes with high importance for the production of medicinal natural products. However, PKS manipulation toward the biosynthesis of polyketide derivatives poses long-standing challenges for which the knowledge of their substrate recognition mechanism is a key aspect. Of particular relevance is the selective introduction of artificial building blocks into the biosynthetic pathway. Thus, we addressed the question of how acyltransferase domains within bacterial type I PKS recruit incoming extender units. Biomolecular modeling was used to predict the substrate flexibility of an acyltransferase domain and to analyze the molecular interactions in the active site. The substrate profile was experimentally investigated using differently substituted derivatives of malonyl-SNAC. Based on these results, a modified acyltransferase domain with significantly altered substrate specificity was designed. At present, the engineering of polyketide biosynthesis is limited by the lack of rationalization of the properties of mutated PKS. Our studies indicate that an interdisciplinary approach can efficiently tackle this problem.

EXPERIMENTAL PROCEDURES

MD simulations of WT-AT6 and V295A AT6 with several non-native substrates (Table 1) were performed using our previously reported model of AT6 as template (Sundermann et al., 2013).

After building the models, CHARMM31b1 (Brooks et al., 1983) was employed for energy minimizations. VMD1.9 (Humphrey et al., 1996) was employed to neutralize the system and to solvate it in a box of water with 12 Å distance between the protein and the walls of the solvent box, as well as for visualization and analysis. Short MD simulations were performed for equilibration before running unconstrained production MD for 30 or 50 ns (NPT ensemble).

All MD simulations were performed using NAMD2.9 (Phillips et al., 2005). The temperature was set to 300 K and a time step of 2 fs was used. The parameters of the substrates were generated using SwissParam (Zoete et al., 2011). The CHARMM22 force field was employed (Mackerell et al., 2004). RMSD values were calculated for the backbone atoms of residues 21–440 of the protein and for all atoms of the substrate.

Plasmids encoding for mutated DEBS3-AT6 were introduced via conjugative plasmid transfer from *Escherichia coli* ET12567/pUZ8002 into *S. erythraea* ΔAT6hyg^R. Resulting clones were cultivated in SM3 medium. *S. erythraea* NRRL-B-24071 and *S. erythraea* ΔAT6hygR carrying a non-mutated DEBS3 expression served as controls. Cultures were supplied with malonic acid derivatives (10–50 mM) and analyzed by LC-ESI-MS and ESI-MS^2 of ethyl acetate extracts (see Supplemental Information).

Synthetic procedures and protocols for the mutagenesis of DEBS AT6 together with analytical data can be found in Klopries et al. (2015).

SUPPLEMENTAL INFORMATION

Supplemental Information includes Computational Section, Feeding Experiments, one table, and three figures and can be found with this article online at http://dx.doi.org/10.1016/j.chembiol.2015.02.008.

AUTHOR CONTRIBUTIONS

Conceptualization: F.S. and E.S.-G.; methodology: F.S., E.S.-G.; formal analysis: K.B.-R. and E.S.-G.; investigation: S. Klopries, K.R.M.K., U.S., S.Y., J.A., and S. Kushnir; writing (original draft): K.B.-R., S. Klopries, E.S.-G., and F.S.; writing (review and editing): E.S.-G. and F.S.; funding acquisition: E.S.-G. and F.S.; supervision: E.S.-G. and F.S.

ACKNOWLEDGMENTS

E.S.-G. acknowledges a Liebig-stipend from the Fonds der Chemischen Industrie and computational time provided by the Max Planck Computing and Data Facility. This work was supported by the Cluster of Excellence RESOLV (EXC 1069) and the Collaborative Research Center SFB1093, both funded by the Deutsche Forschungsgemeinschaft.

Received: October 22, 2014
Revised: January 16, 2015
Accepted: February 23, 2015
Published: October 29, 2015

REFERENCES

Bao, X., Zhao, Q., Yang, T., Fung, Y.M.E., and Li, X.D. (2013). A chemical probe for lysine malonylation. Angew. Chem. Int. Ed. Engl. *52*, 4883–4886.

Bravo-Rodriguez, K., Ismail-Ali, A.F., Klopries, S., Kushnir, S., Ismail, S., Fansa, E.K., Wittinghofer, A., Schulz, F., and Sanchez-Garcia, E. (2014). Predicted incorporation of non-native substrates by a polyketide synthase yields bioactive natural product derivatives. Chembiochem *15*, 1991–1997.

Brooks, B.R., Bruccoleri, R.E., Olafson, B.D., States, D.J., Swaminathan, S., and Karplus, M. (1983). CHARMM: a program for macromolecular energy, minimization, and dynamics calculations. J. Comput. Chem. *4*, 187–217.

Hertweck, C. (2009). The biosynthetic logic of polyketide diversity. Angew. Chem. Int. Ed. Engl. *48*, 4688–4716.

Humphrey, W., Dalke, A., and Schulten, K. (1996). VMD: visual molecular dynamics. J. Mol. Graph. *14*, 33–38.

Kazlauskas, R.J. (2005). Enhancing catalytic promiscuity for biocatalysis. Curr. Opin. Chem. Biol. *9*, 195–201.

Klopries, S., Sundermann, U., and Schulz, F. (2013). Quantification of N-acetylcysteamine activated methylmalonate incorporation into polyketide biosynthesis. Beilstein J. Org. Chem. *9*, 664–674.

Klopries, S., Bravo-Rodriguez, K., Koopmans, K.R.M., Sundermann, U., Yahiaoui, S., Arens, J., Kushnir, S., Sanchez-Garcia, E., and Schulz, Frank (2015). Data in support of substrate flexibility of a mutated acyltransferase domain and implications for polyketide biosynthesis. Data Brief. http://dx.doi.org/10.1016/j.dib.2015.09.052.

Koryakina, I., McArthur, J., Randall, S., Draelos, M.M., Musiol, E.M., Muddiman, D.C., Weber, T., and Williams, G.J. (2012). Poly specific trans-acyltransferase machinery revealed via engineered acyl-CoA synthetases. ACS Chem. Biol. *8*, 200–208.

Koryakina, I., McArthur, J.B., Draelos, M.M., and Williams, G.J. (2013). Promiscuity of a modular polyketide synthase towards natural and non-natural extender units. Org. Biomol. Chem. *11*, 4449–4458.

Kushnir, S., Sundermann, U., Yahiaoui, S., Brockmeyer, A., Janning, P., and Schulz, F. (2012). Minimally invasive mutagenesis gives rise to a biosynthetic polyketide library. Angew. Chem. Int. Ed. Engl. *51*, 10664–10669.

Kwan, D.H., Sun, Y., Schulz, F., Hong, H., Popovic, B., Sim-Stark, J.C.C., Haydock, S.F., and Leadlay, P.F. (2008). Prediction and manipulation of the stereochemistry of enoylreduction in modular polyketide synthases. Chem. Biol. *15*, 1231–1240.

Lau, J., Fu, H., Cane, D.E., and Khosla, C. (1999). Dissecting the role of acyltransferase domains of modular polyketide synthases in the choice and stereochemical fate of extender units. Biochemistry *38*, 1643–1651.

Mackerell, A.D., Feig, M., and Brooks, C.L. (2004). Extending the treatment of backbone energetics in protein force fields: limitations of gas-phase quantum mechanics in reproducing protein conformational distributions in molecular dynamics simulations. J. Comput. Chem. *25*, 1400–1415.

Mo, S., Kim, D.H., Lee, J.H., Park, J.W., Basnet, D.B., Ban, Y.H., Yoo, Y.J., Chen, S.-w., Park, S.R., and Choi, E.A. (2010). Biosynthesis of the allylmalonyl-CoA extender unit for the FK506 polyketide synthase proceeds through a dedicated polyketide synthase and facilitates the mutasynthesis of analogues. J. Am. Chem. Soc. *133*, 976–985.

Morley, K.L., and Kazlauskas, R.J. (2005). Improving enzyme properties: when are closer mutations better? Trends Biotechnol. *23*, 231–237.

Newman, D.J., and Cragg, G.M. (2012). Natural products as sources of new drugs over the 30 years from 1981 to 2010. J. Nat. Prod. *75*, 311–335.

Oliynyk, M., Brown, M.J.B., Cortés, J., Staunton, J., and Leadlay, P.F. (1996). A hybrid modular polyketide synthase obtained by domain swapping. Chem. Biol. *3*, 833–839.

Phillips, J.C., Braun, R., Wang, W., Gumbart, J., Tajkhorshid, E., Villa, E., Chipot, C., Skeel, R.D., Kalé, L., and Schulten, K. (2005). Scalable molecular dynamics with NAMD. J. Comput. Chem. *26*, 1781–1802.

Quade, N., Huo, L., Rachid, S., Heinz, D.W., and Müller, R. (2012). Unusual carbon fixation gives rise to diverse polyketide extender units. Nat. Chem. Biol. *8*, 117–124.

Reetz, M.T. (2013). The importance of additive and non-additive mutational effects in protein engineering. Angew. Chem. Int. Ed. Engl. *52*, 2658–2666.

Sundermann, U., Bravo-Rodriguez, K., Klopries, S., Kushnir, S., Gomez, H., Sanchez-Garcia, E., and Schulz, F. (2013). Enzyme-directed mutasynthesis: a combined experimental and theoretical approach to substrate recognition of a polyketide synthase. ACS Chem. Biol. *8*, 443–450.

Weissman, K.J., and Leadlay, P.F. (2005). Combinatorial biosynthesis of reduced polyketides. Nat. Rev. Micro *3*, 925–936.

Zoete, V., Cuendet, M.A., Grosdidier, A., and Michielin, O. (2011). SwissParam: a fast force field generation tool for small organic molecules. J. Comput. Chem. *32*, 2359–2368.

